American Journal of Pathology, Vol. 163, No. 5, November 2003

Animal Model

Viable Mouse Models of Acid β-Glucosidase Deficiency

The Defect in Gaucher Disease

You-Hai Xu,* Brian Quinn,* David Witte,† and Gregory A. Grabowski*

From the Divisions of Human Genetics and Pathology,† Cincinnati Children's Hospital Research Foundation, Cincinnati, Ohio*

Gaucher disease is an autosomal recessively inherited disease caused by mutations at the acid β-glucosidase (GCase) locus (*GBA*). To develop viable models of Gaucher disease, point mutations (pmuts), encoding N370S, V394L, D409H, or D409V were introduced into the mouse GCase (*gba*) locus. DNA sequencing verified each unique pmut. Mutant GCase mRNAs were near wild-type (WT) levels. GCase activities were reduced to 2 to 25% of WT in liver, lung, spleen, and cultured fibroblasts from pmut/pmut or pmut/null mice. The corresponding brain GCase activities were ~25% of WT. N370S homozygosity was lethal in the neonatal period. For the other pmut mice, a few storage cells appeared in the spleen at ≥7 months (D409H or D409V homozygotes) or ≥1 year (V394L homozygotes). V394L/null, D409H/null, or D409V/null mice showed scattered storage cells in spleen at ~3 to 4 months. Occasional storage cells (sinusoidal cells) were present in liver. In D409V/null mice, large numbers of Mac-3-positive storage cells (ie, macrophages) accumulated in the lung. Glycosphingolipid analyses showed varying rates of progressive glucosylceramide accumulation in visceral organs of pmut/pmut or pmut/null mice, but not in brain. These GCase-deficient mice provide tools for gaining insight into the pathophysiology of Gaucher disease and developing improved therapies. *(Am J Pathol 2003, 163:2093–2101)*

Gaucher disease, an autosomal recessive trait, is the most common lysosomal storage disease.[1] Defective activity of acid β-glucosidase (glucocerebrosidase, GCase, EC3.2.1.45) in all cells leads to the various clinical phenotypes. Over 200 mutations at the human GCase locus (*GBA*) have been defined in affected patients.[1] The human disease phenotypes are highly variable, but all exhibit hepatosplenomegaly and usually bone involvement. Distinct variants have been described that do or do not primarily affect the central nervous system.[1–3] The macrophage is the primary cell in visceral tissues involved in all variants, but neuronal cell death is the major pathology in the neuronopathic variants.[4,5] The molecular bases have not been elucidated for the phenotypic variation, nor the presence or absence of neuronopathic diseases.

Genotype/phenotype correlations in human Gaucher disease also are limited.[6,7] The presence of at least one N370S allele in affected patients is associated universally with type 1, non-neuronopathic disease. N370S homozygosity is associated with less severe phenotypes than some heteroallelic states, eg, N370S/null. In contrast, patients with the D409H/D409H genotype have a nearly unique phenotype that includes neuronopathic disease, hydrocephalus, and cardiac valvular and aortic calcification.[8] Homozygous patients with V394L or D409V alleles have not been described, but the mutations have been observed in heteroallelic patients.[9,10] The N370S and V394L enzymes have significant residual activity with very similar *in vitro* kinetic properties.[11] The D409H and D409V enzymes are catalytically defective, unstable, and susceptible to proteolytic digestion in insect cell expression systems.[11] The absence of GCase activity in humans is not compatible with sustained survival in the postnatal period.[12–14] Similarly, the targeted disruption of mouse GCase (mGCase) locus (*gba*) leads to a mouse that survives for only a few hours after birth because of a skin permeability abnormality.[15,16] Absence of a viable animal model has limited progress in understanding the pathogenesis of Gaucher disease.

Supported by a grant from the NIH to GAG (DK 36729).

Accepted for publication July 17, 2003.

Address reprint requests to Gregory A. Grabowski, M.D., Cincinnati Children's Hospital Research Foundation, Division of Human Genetics, 3333 Burnet Avenue, Cincinnati, Ohio 45229-3039. E-mail: greg.grabowski@cchmc.org.

In comparison, animal models do exist for a variety of other lysosomal storage diseases and these have greatly facilitated pathophysiologic and natural history studies. These analogues of the human diseases have lead to characterization of visceral and central nervous system (CNS) involvement, and have provided useful tools for a therapeutic endeavors.[17–19] Many of the lysosomal diseases lack spontaneously occurring animal models and targeted disruption or "knock-in" techniques have been used to alter the genes in mice to create such models.[16,20–23] In some, the resultant phenotypes have approximated the human disease. Farber disease (ceramidase deficiency) and Gaucher disease (GCase deficiency) have been notable exceptions.[15,23] These two related diseases both involve defects in the final sequential steps in the degradation of higher gangliosides and gluco-based sphingolipids to sphingosine and fatty acids in the lysosome.[24] The ceramidase null mouse has an early embryonic lethal phenotype as a result of aggressive apoptosis of the fertilized zygote.[23] The *gba* knock-out model exhibits defective skin permeability and rapid demise shortly after birth.[15] Similar early lethal phenotypes were found in the "knock-in" mice bearing the L444P alleles.[16] In humans, L444P/L444P homozygosity is compatible with survival, albeit with a propensity to develop CNS disease.[25,26] Thus, unlike the mouse models for other lysosomal diseases, the knock-out mouse for Gaucher disease has not proved highly useful for detailed pathophysiologic studies.

In an effort to develop Gaucher disease mouse models, point mutations were introduced into *gba* that would result in differential levels of GCase residual activities, potentially leading to different phenotypes. The phenotypic, histological, and biochemical abnormalities are presented for these viable mGCase mutant models.

Materials and Methods

Materials

The following were from commercial sources: culture media/antibiotics, random labeling kit, Trizol reagent, Superscript first-strand synthesis system, baculovirus expression system (pBlueBac4.5 vector, and *Sf9* and *Sf*21 insect cells) and TA cloning vector pCRII (Invitrogen, Carlsbad, CA); 4-methyl-umbelliferyl-β-*D*-glucopyranoside (4MU-Glc; Biosynth AG, Switzerland); sodium taurocholate and Protease Inhibitor Cocktail (Calbiochem, La Jolla, CA); Triton X-100 and primulin (Sigma, St. Louis, MO); pET21a vector and *E. coli* BL21 strain system (Novagen, Madison, WI); TOTALLY RNA kit (Ambion, Austin, TX); restriction enzymes (New England Biolab, Boston, MA); Quick-Change kit (Stratagene, CA); PVDF membrane (Millipore, Bedford, MA); alkaline phosphates (AP)-conjugated goat anti-rabbit IgG and AP-developing reagents A & B (Bio-Rad, Hercules, CA); rat anti-mouse Mac-3 monoclonal antibody (Pharmingen, Palo Alto, CA); ABC Vectastain (Vector Laboratory, Burlingame, CA); [^{32}P]-dCTP (PerkinElmer Life Sciences, Boston, MA); and the *gba* null mouse[15] was from Jackson Laboratories (Stock No. 002594).

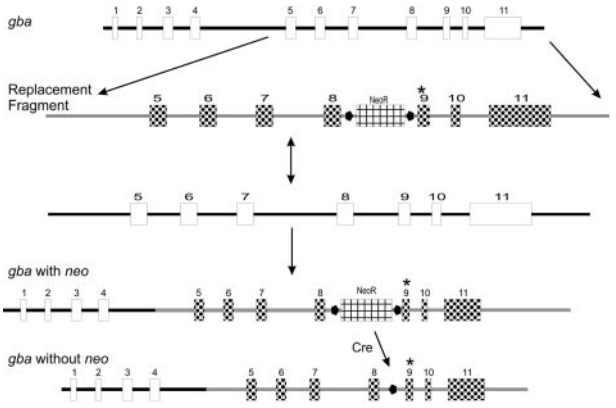

Figure 1. Mouse *gba* targeting strategy. The WT *gba* is shown at the top. The replacement fragment from the targeting construct (second line) contained exons 5 to 11, parts of intron 4 and the 3′ flanking region, and a floxed *neo* selection marker in intron 8. The fourth line shows the resultant recombination with *gba* (*gba* with *neo*) and, following *cre* excision of *neo* (*gba* without *neo*) the recombined allele containing one loxP (⬟) site and the individual exon 9 mutations (*).

Targeting Constructs and Genotyping

After specifying the point mutations and construct characteristics, targeting construct development, embryonic stem (ES) cell homologous recombination and injection, and breeding of chimeras for each mutant allele with or without *neo* were under a fee-for-service contract (Lexicon Corp., Houston, TX). Targeting vectors contained all of exons 5 to 11 and part of intron 4 and the 3′ flanking region of *gba* (Figure 1). The single base substitutions c.A1249G, c.G1320C, c.G1365C, or c.A1366T in exon 9 were specified to encode N370S, V394L, D409H, and D409V. The nucleotide numbering was based on the mGCase mRNA/cDNA sequence (GenBank Accession No. M24119).[27] ES cells were from the 129/SvEvBrd stain. For the majority of these mice, the PGK*neo*-loxP sequence was removed using a protamine promoter-driven *cre* recombinase transgene in spermatogonia of male chimeric mice, thereby leaving only a 94-bp loxP junction sequence in intron 8 of sperm. Transmitting mice were crossed into C57BL/6 to generate heterozygotes bearing the point-mutated alleles. The mutations in these mice were verified by sequencing the intron 8 and exon 9 regions and the entire mGCase cDNA from cellular mRNA of homozygous mice. The genomic fragments were generated by PCR using the 5′ primer mGC4996F (5′-CACAGATGTGTATGGCCATCGG-3′, intron 8 region) and the 3′ primer mGC5387R (5′-CTGAAGTGGCCAAGATGGTAG-3′, end of exon 9). This pair of primers generated a 391-bp fragment from wild-type (WT) *gba* DNA and a 485-bp fragment (391 + 94-bp lox-P junction sequence) from all point-mutated *gba* DNA. PCR was performed at 94°C, 1 minute; 58°C, 1 minute; 72°C, 1 minute for 35 cycles, and then, 72°C, 7 minutes for one cycle. For cDNA synthesis the 5′ primer was 5′-GGCCGGAATTCCTCCAGTTTCCAAGATC-3′ and the 3′ primer was 5′-GTGCTAAGTCTAGATGCCTGCTCAGG-3. The mGCase

full-length cDNAs were cloned into pCRII from point-mutated or WT homozygotes. The mutated and WT homozygotes DNA sequencing showed only the created point mutation from each respective allele.

Creation of the *gba* null allele by insertion of the *neo* containing vector sequence (~1850 bp) resulted in an additional deletion of genomic nucleotides g.5330 to g.5728 in exons 9 to 10 (Jackson Laboratory Stock No. 002594).[15] This was determined by sequencing the allele and development of the following PCR primers for genotyping the *gba* null/WT mice: forward primer 1 (mGC5223F) located in *gba* exon 9 (5′-GAACCTCCTTTACCACGTAACTGG-3′); reverse primer 2 in the knock-out vector (5′-GGCCTACCCGCTTCCATTGCT-3′); and reverse primer 3 (mGC5765R) located in *gba* exon 10 (5′-GTGCTCTCACTGGCCACCAACG-3′). PCR with primers 1 and 3 generated ~550-bp fragment from the WT allele of the null/WT mouse and primers 1 and 2 generated about ~430-bp fragment from the "knock-out" allele. PCR was performed at 94°C for 1 minute, 58°C 1 minute, 72°C 1 minute for 35 cycles, and then, 72°C, 7 minutes for one cycle. The PCR products were verified by sequencing.

Northern Blots

Total RNA from cultured skin fibroblasts of WT or point-mutated mice was isolated using Trizol reagent. For isolation of tissue RNAs, liver, spleen, lung, and brain tissues were immediately processed using the TOTALLY RNA kit. Total poly(A) RNA was isolated using Oligotex (Qiagen). Northern analyses then were conducted as described.[28] Signals were normalized to GAPDH mRNA.[29] Quantification was by densitometry (Storm 860 PhosphoImager, Amersham-Pharmacia Pharmacia Biotech).

Expression of mGCase and Activity Assays

The full length mGCase cDNA was cloned into and expressed from the pET2la vector. The resultant GCase was purified by SDS-PAGE (12.5%) and electro-eluted.[30] Rabbit anti-mGCase antibodies were raised as described.[31] For characterizing mouse WT and mutant GCase activities, the full length (1.6 kb) WT mGCase cDNA was re-cloned into pBlueBac4.5, recombinant virus isolated, and mGCase expressed in *Sf21* insect cells. The N370S, V394L, D409H, and D409V mutant templates were generated by mutagenesis in pBlueBac4.5 on the WT background using the Quick-Change kit and verified by sequencing. Transfections, cell culture, selection of recombinant virus, and plaque assays were performed as described.[32] mGCases were isolated from serum-free medium surrounding *Sf*21cells that had been infected at MOI 5 to 10. The medium contained DTT (1 mmol/L). Enzyme assays, conduritol B epoxide inhibition (CBE), and CRIM-specific activities were as described for the hGCase.[11,33] For tissue mGCase activities, assay mixtures were preincubated in the presence and absence of CBE (1 mmol/L) for 40 minutes (37°C). The substrate (4MU-Glc) was added and the reactions were stopped after an additional 30 minutes of incubation (37°C).[11]

Tissue Lipid Analyses

Tissue samples (~100 mg wet weight) were added to H_2O (0.6 ml) and methanol (2 ml), homogenized (Power-Gen 35, Fisher Scientific), and then chloroform (1 ml) was added. The samples were shaken (> 15 minutes) and centrifuged (5 minutes, 1000 × *g*). The pellet was re-extracted with H_2O (0.7 ml) and chloroform/methanol (3 ml, 1/2 v/v). The combined organic phase supernatants were centrifuged (10 minutes, 7,000 × *g*), transferred to fresh tubes, and dried under N_2.[34] Extracts were resuspended in chloroform/methanol/water (15 ml, 60/30/4.5, v/v/v) and desalted on Sephadex G-25 (0.8 × *g*).[35] These samples were subjected to alkaline methanolysis[36] and desalted. Relative proportions of lipids from ~100 mg (wet weight) of tissue samples were determined by thin-layer chromatography with borate impregnated plates[37] (TLC, 10 cm^2 Merck HPTLC silica gel 60, 200 μm). Plates were developed in chloroform/methanol/water (65/25/4, v/v/v). Lipids were visualized with primulin spray (100 mg/L in 80% acetone) and blue fluorescence scanning (Storm 860, Amersham Pharmacia Biotech).

Histological Studies

Mutant and WT mice were sacrificed by age groups. The major organs (liver, spleen, lung, brain, bone marrow, and skin) were collected, fixed in 10% buffered formalin, embedded in paraffin, sectioned, and stained with hematoxylin and eosin (H&E) for light microscopic studies. For Mac-3 monoclonal antibody staining, tissues were fixed with 4% paraformaldehyde in PBS, pH 7.4. Sections were incubated with rat anti-mouse Mac-3 monoclonal antibody in PBS containing 5% goat serum for 1 hour at 37°C. Biotinylated goat anti-rat IgG was used as the reporter. Detection was performed using ABC Vectastain and DAB peroxidase substrate according to manufacturer's instruction.

Results

Creation of missense mutations in *gba*. *gba* point mutations encoding for N370S, V394L, D409H, and D409V were created (Figure 1) and appropriate homologous recombination was verified by Southern blotting (data not shown). Germ-line transmission of mutations encoding N370S, V394L, D409H, or D409V was verified and each chimeric variant was crossed into C57BL/6 mice. The homozygotes for the point-mutated *gba* mice reported here represent a mixture of ~50% C57B/6 and ~50% 129/SvEvBrd. The desired point mutation in each mouse line was verified by sequencing intron 8 and exon 9 regions of *gba* and the entire mGCase cDNA (see below). The diagnostic PCR analyses showed a 391-bp fragment from the WT *gba* locus (Figure 2, bottom band) or a

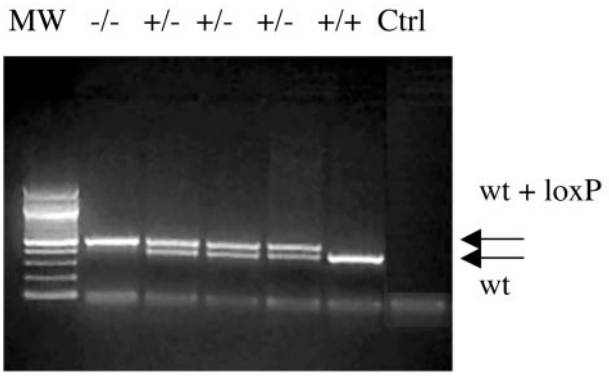

Figure 2. Genotype analyses for *gba* point mutations. A 391 bp PCR fragment from WT (**bottom arrow**) or a 485-bp PCR fragment (391+loxP, **top arrow**) from point-mutated *gba* mice. The genotypes are indicated above each **lane**. +/+, WT homozygote; +/−, heterozygote (V394L, D409H, and D409V); and −/−, homozygote (eg, D409V). Ctrl is the PCR control without template DNA. MW = size standards.

485-bp fragment from the mutated allele (Figure 2, top band). This strategy was used for mouse genotyping.

Homozygotes for the point mutations containing *neo* (see Figure 1; ie, N370S+*neo*/N370S+*neo* or V394L+*neo*/V394L+*neo*) and the N370S homozygotes (N370S-*neo*/N370S-*neo*) died within 24 hours of birth. The dead pups resembled null/null pups,[15] and had red, wrinkled, dry skin that was indicative of disruption of the skin permeability barrier. Cultured skin fibroblasts from the mice that bore *neo*+ alleles had no detectible mature mGCase mRNA or mGCase activity. Homozygotes for the V394L, D409H, or D409V survived to at least 58 to 78 weeks, and were fertile. Additional phenotypes were obtained by producing V394L/null, D409H/null, or D409V/null mice by crossing homozygote point mutants with null/WT mice. Total cellular RNA from cultured skin fibroblasts of point-mutated mice was subjected to RT-PCR to generate cDNAs for sequencing. The sequence of full-length GCase cDNAs showed only the specified substitutions that corresponded to alleles encoding N370S, V394L, D409H, or D409V. These were the only differences from the cDNA sequence of simultaneously sequenced mGCase cDNAs from homozygous WT littermates.

Table 2. CRIM-Specific Activity of Mutant mGCases Expressed in Insect Cells

Source	Relative GCase activity
WT	100%
N370S	15.4 ± 5.1%
V394L	12.4 ± 3.4%
D409H	12.9 ± 3.5%
D409V	21.6 ± 4.8%

GCase activity assays were conducted with mGCases harvested from media of *Sf*21 insect cells infected with the appropriate recombinant baculovirus. CRIM amounts were determined by densitometric scans of immunoblots. Values ± SD were from three determinations.

Characterization of GCase mRNA, Protein, and Enzyme Activities from gba *Mutated Mice*

mGCase RNA levels in fibroblasts and tissues were quantified using Northern hybridizations. [^{32}P]-GCase RNA signals were normalized to those hybridized with [^{32}P]-GAPDH RNA on the same membranes. The mGCase mRNA levels in WT cells/tissues were set to 100%. The levels of mGCase mRNA from cultured skin fibroblasts of homozygous point-mutated mice (N370S, V394L, D409H, or D409V) were within a twofold range (63 to 115%) of that in WT (relative to GAPHD). The levels of mGCase RNAs from liver of homozygous point-mutated or point-mutant/null mice also ranged from 50 to 100% of WT. Similar results were obtained from the Northern analyses of spleen and brain. In comparison, no mature mGCase RNA was detected in skin fibroblasts from the null/null mice. A slower migrating band (~5.7 kb) from null/null mouse mRNAs hybridized with a *neo* probe indicating that the RNA was disrupted by the inserted sequence.

In general, for homozygotes the residual mGCase *in vitro* activity levels in tissue and fibroblasts were in the following order: WT>V349L>N370S (fibroblasts only)>D409H>D409V (Table 1). The lowest GCase activities (2.5 to 6.4% of WT) were in liver. Slightly higher levels were in spleen (4.5 to 10.9% of WT), and in lung (4.0 to 7.7% of WT). In comparison, the residual activity in brain was higher (21.4 to 27.8% of WT). The residual activities of the point-mutant/null mice were lower than the corresponding homozygotes. The presence of neutral

Table 1. GCase Activity in Tissues and Skin Fibroblasts of Point-Mutated Mice*

	Liver (%)	Spleen (%)	Brain (%)	Lung (%)	Fibroblasts (%)
WT/WT	100	100	100	100	100
N370S/N370S	N/A†	N/A†	N/A†	N/A†	12.8 ± 2.3
V394L/V394L	4.0 ± 1.4	10.9 ± 2.7	27.4 ± 3.6	7.0 ± 1.4	25.1 ± 6.3
V394L/null	6.4 ± 0.7	6.2 ± 1.2	23.0 ± 4.5	7.7 ± 1.4	12.8 ± 3.6
D409H/D409H	5.4 ± 2.4	9.3 ± 2.2	27.8 ± 6.8	6.7 ± 0.8	7.7 ± 1.5
D409H/null	5.7 ± 0.7	4.5 ± 2.0	23.3 ± 3.59	4.2 ± 0.7	3.2 ± 1.2
D409V/D409V	2.5 ± 0.9	6.2 ± 2.7	22.5 ± 3.8	5.4 ± 2.2	4.4 ± 0.9
D409V/null	3.9 ± 0.4	6.8 ± 3.2	21.4 ± 1.6	4.0 ± 1.3	3.2 ± 0.8
Null/null	N/A†	N/A†	N/A†	N/A†	1.0 ± 0.2

*GCase activity assays (± SD) were conducted in presence of the GCase irreversible inhibitor CBE (Materials and Methods). Assays were performed with samples from three to five individual animals.

†NA, N370S/N370S, and null/null died shortly after birth and assays on tissue extracts were not available.

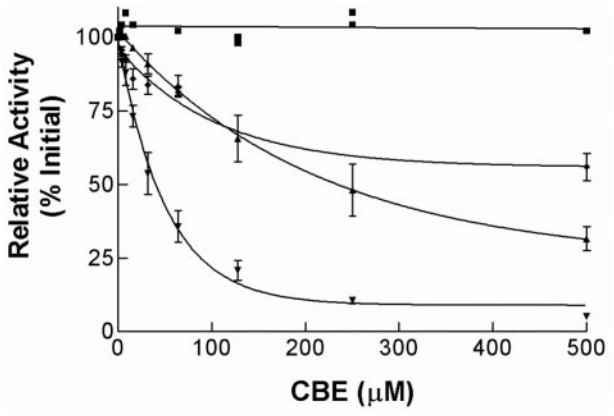

Figure 3. CBE inhibition of mouse N370S and V394L mGCases: WT (▼), V394L (♦) and N370S (▲) mGCase were harvested from media of *Sf21* cells infected with the desired recombinant baculovirus. The enzymes were delipidated and dialyzed before being incubated (30 minutes; 37°C) with conduritol B epoxide (CBE, 1 to 500 μmol/L) and 4MU-Glc (4 mmol/L). The control sample (■) was from media of uninfected *Sf*21 cells.

(non-CBE inhibitable) activity in all tissues, except fibroblasts, may have obscured perfect correlations even in the presence of CBE.[38] Tissues for enzyme assays of N370S/N370S, N307S/null, or null/null were not available due to the lethal phenotype.

The recombinant mGCases (WT, N370S, V394L, D409H, and D409V) were expressed using the baculovirus system. Each mGCase activity was determined in culture medium of infected *Sf21* cells. The specific activities relative to cross-reacting immunological material (CRIM) were determined for each point-mutated mGCase (Table 2). These values varied between ~12 and 22% of WT, indicating an eight- to fivefold decrease catalytic function (ie, k_{cat}) for the mutant proteins. The CBE IC_{50} values for WT, and the N370S and V394L mGCases differed by about fivefold (Figure 3). The results showed that the N370S and V394L mGCases and hGCases had similar *in vitro* kinetic properties.[11]

Phenotypic, Histological, and Lipid Characterization of gba *Point-Mutated Mice*

Mice homozygous or compound heterozygous for *gba* point mutations, except N370S, appear phenotypically normal and have survived as follows: >78 weeks for V394L/V394L, >68 weeks for D409H/D409H, and >66 weeks for D409V/D409V. All of the point-mutant/null mice lived >42 weeks. The total life-spans of these mice could be >75 weeks, but were foreshortened by sacrifice. All mice have grossly normal behavior, reproduce and show no gross evidence of CNS abnormalities. The liver weight ranged from 5.2 to 6.1% of body weight (n = 40; WT = 5.2%, n = 12). The splenic weight ranged from 0.2 to 0.4% of body weight (n = 40; WT = 0.33%, n = 12).

The histologies of the liver, spleen, lung, and bone marrow were evaluated by H&E stained tissue sections under light microscopy. The spleen was involved in all mice. Storage cells (Gaucher cells) appeared in small numbers in spleen at ≥7 months (D409H/D409H or D409V/D409V) or ≥1 year (V394L/V394L) (Figure 4). In mice with the V394L/null, D409H/null, or D409V/null genotypes, storage cells appeared ~3 to 4 months earlier than in the corresponding homozygotes. In D409V/null, large numbers of storage cells also appeared in lung (Figure 5, top) and a few scatter cells in liver at 3 months. These storage cells stained positive for the cell surface antigen Mac-3 (Figure 5, bottom). No obvious storage cells were found in other tissues, ie, brain, kidney, or bone marrow. No differences in the phenotypes or histology of heteroallelic mice, ie, V394L/N370S, were detected when compared to that in the respective homozygotes or point-mutant/null mice. This indicated a lack of *in vivo* negative interactive effects between the various point-mutated proteins.

Accumulations of glucosylceramide were present in various tissues. At 6.5 months, D409V/null mice had glucosylceramide accumulation in liver, lung, and spleen (~4xWT), but not in brain (Figure 6). The D409V/D409V,

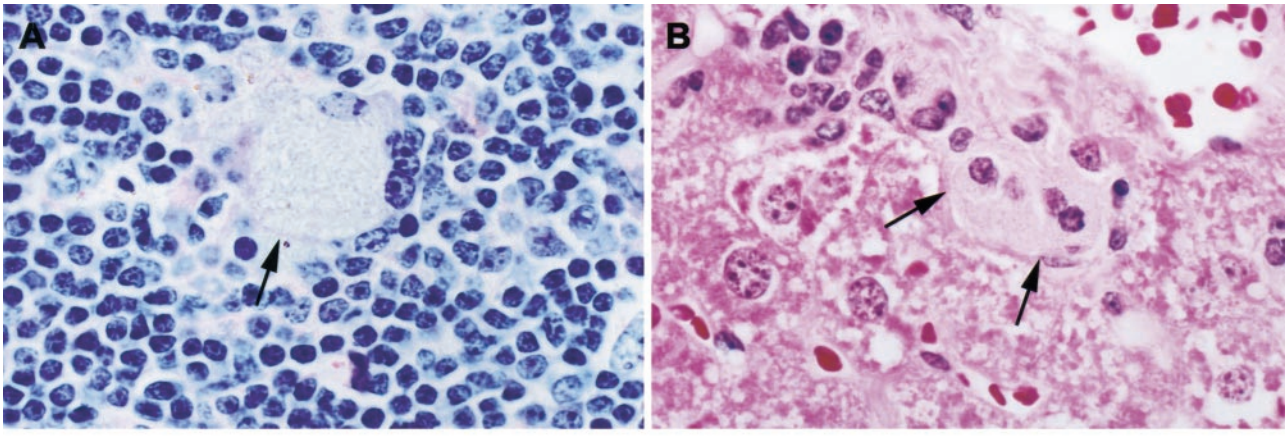

Figure 4. Storage cells in spleen and liver of *gba* point-mutated mice. **A:** Representative samples from spleen of D409V/null mice. A large storage cell (**arrow**) is illustrated with prominent amounts of pale staining vacuolated cytoplasm. (H&E, magnification, ×400). **B:** A representative section from liver. A small cluster of pale staining storage cells are illustrated in the sinusoidal space (H&E, magnification, ×400).

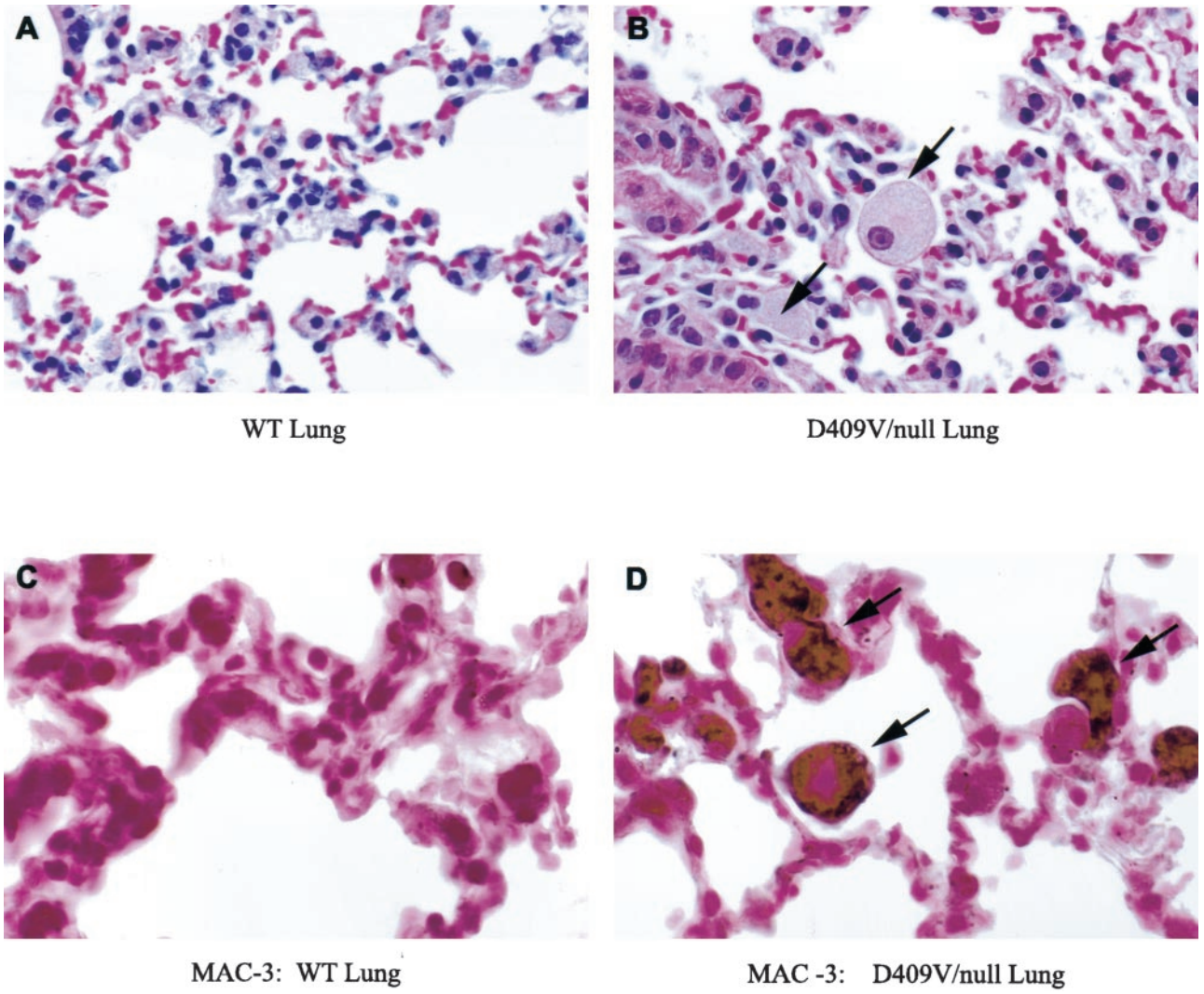

Figure 5. Storage cell staining with Mac-3. **A:** Section of wild-type lung with no accumulation of storage cells in the alveolar spaces. **B:** D409V/null lung with large storage cells (**arrows**) in the alveolar space. **C:** Wild-type lung stained for Mac-3. **D:** Mac-3 staining of lung from the D409V/null mouse indicating macrophage origin of the storage cells. Magnification: ×165 (**A**), ×250 (**B**), ×350 (**C** and **D**).

D409H/D409H, and D409H/null mice all had a smaller amount of accumulated glucosylceramide (~2- to 4-fold) in these tissues at comparable ages. In 13-month V394L/V394L and 9-month V394L/null mice lesser glucosylceramide accumulations were observed in liver, spleen, and/or lung compared to the other variants (Figure 6). None of the mutant mice showed increased glucosylceramide in brain.

Discussion

Transgenic and "knock-out" mice have provided powerful tools to investigate the pathophysiology and molecular bases of a variety of human diseases. The lack of a viable mouse model in Gaucher disease has been a significant impediment to understanding some of the complexities of this disease including genotype/phenotype correlation, general, or tissue-specific pathophysiologies, and the development of new therapeutic approaches. The knock-out mouse (*gba*-null) and L444P-like mutations resulted in neonatal death.[15,16] A potential confounder in such mice was the insertion of large amounts of extraneous (*neo* and other) sequences in introns or the 3′ region of *gba*.[15,16] Indeed the V394L+*neo* homozygotes had a phenotype similar to the null/null and "L444P-like" homozygotes. These studies indicated the need to develop genetically altered mice without significant extraneous sequences. An interesting complex mouse model was developed by combining the L444P homozygote with a substrate supply reduction (heterozygote for the glucosylceramide synthase knock-out).[39] These mice lived for more than 1 year, but did not display a storage phenotype, although inflammation was noted in several tissues. Such inflammation was not present in the mutant mice presented here.

To develop improved mouse models for Gaucher disease, four individual GCase point mutations were introduced into *gba* using the cre-loxP system to remove the intron 8 *neo* selection marker.[40] Homozygotes for V394L, D409H, and D409V had no gross phenotypic abnormal-

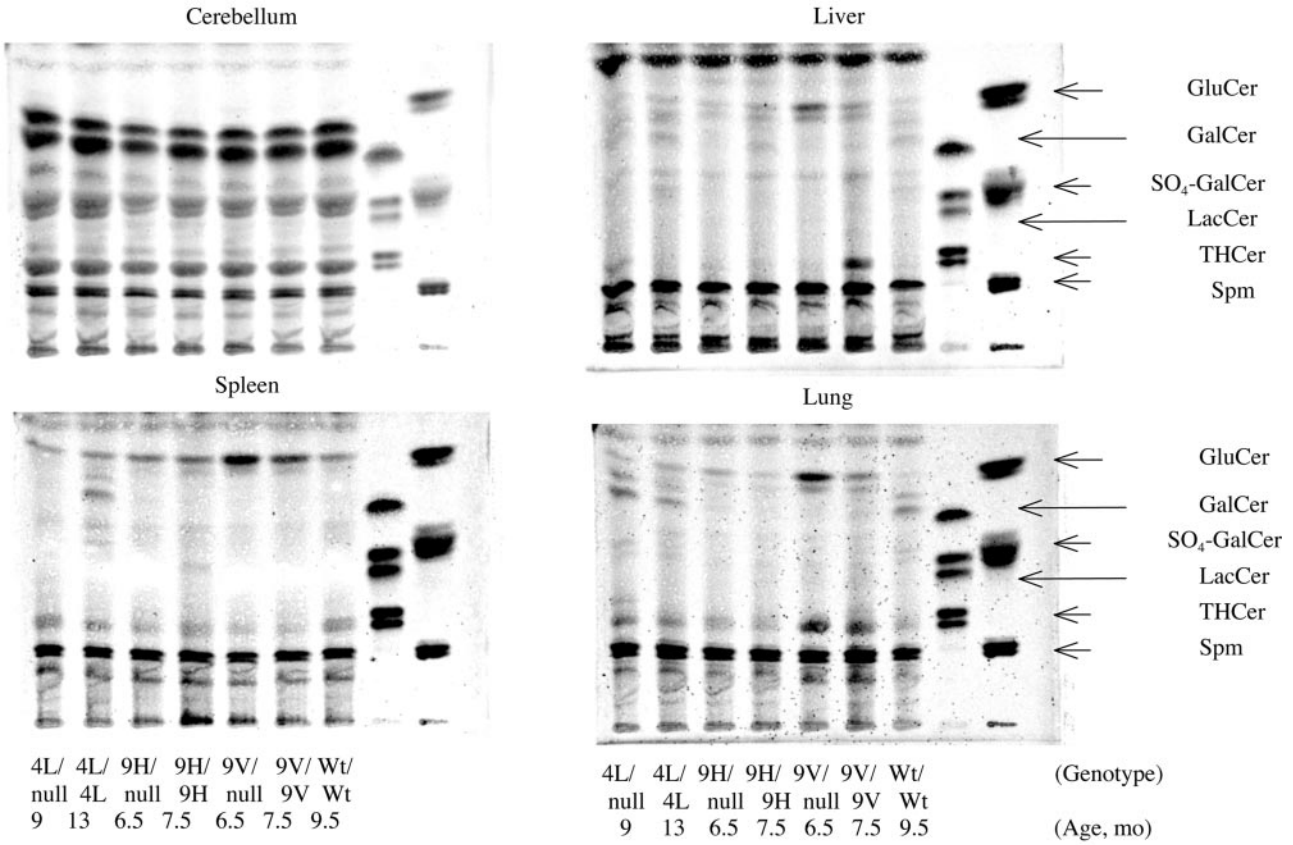

Figure 6. Glycosphingolipid (GSL) profiles from various tissue of point-mutated *gba* mice. Cerebellum, liver, spleen, and lung (~100 mg wet weight) were from *gba* mutant mice at various ages. The tissues were processed for thin-layer chromatography. The genotypes and ages are indicated only on the **bottom** for clarity of presentation. Migration standards for of sphingolipids are on the right: GluCer, glucosylceramide; GalCer, galactosylceramide; SO_4-GalCer, sulfogalactosylceramide; LacCer, lactosylceramide; THCer, ceramide trihexoside; Spm, sphingomyelin. The borate-impregnated plates were developed in chloroform/methanol/water (65/25/4) using borate-impregnated plates. Mature WT mice showed little variation in GSL levels in the respective tissues within the time frame of these experiments.

ities, were fertile, and reproduced. The residual activity in major organs of these mice was low, and few macrophage storage cells were in the spleen at ≥7 months in D409H and D409V homozygotes and ≥1 year in V394L homozygotes. Concomitantly, in these homozygous mice only small amounts of glucosylceramide accumulated. In comparative studies of recombinant mouse WT or mutant (eg, N370S) GCases, or mGCases from tissues (D409H, D409V, or V394L), the mutant enzymes had similar properties to the corresponding hGCases.[11] These observations indicate different effects of homologous mutations in mice and humans.

Mice with greater reductions in residual activity were developed by crossing the GCase point-mutated and null mice. Compared to the corresponding homozygotes, these compound heterozygotes developed more and earlier storage cells and glucosylceramide accumulation. Large numbers of storage cells and glucosylceramide in the lungs of the D409V/null mice and the predilection for storage material in the spleen indicates differential substrate supplies and fluxes in various tissues. Such results provide support for thresholds of residual activities/altered substrate fluxes that dictate phenotypic development. This threshold level for glucosylceramide flux depends on the overall flux through the GSL degradative and biosynthetic pathways.[41] Recent studies of *gba*$^{L444P/L444P}$Ugcg$^{+/KO}$ mice, ie, homozygous for a L444P alleles and heterozygous for a glucosylceramide synthase knock-out allele, also support such thresholds.[39] Reducing synthesis of glucosylceramide changed the phenotype to mice that live beyond a year without storage. Theoretically, glucosylceramide flux through the GSL pathway depends on influx and efflux and the Ugcg$^{+/KO}$ mice would have reduced glucosylceramide storage.[16,39] This model supports the importance of substrate flow through the pathway in determining the threshold level of substrate flux that influences phenotypic development.

The *gba*$^{L444P/L444P}$Ugcg$^{+/KO}$ and the point-mutated mice developed here differ significantly. Importantly, the point-mutated mice have storage of glucosylceramide and storage cells whereas the *gba*$^{L444P/L444P}$Ugcg$^{+/KO}$ did not. Certainly, the viability of the latter mice depended on the presence of the heterozygous state for a knock-out of glucosylceramide synthase, which decreased the level of substrate. In addition, these *gba*$^{L444P/L444P}$Ugcg$^{+/KO}$ mice were against a mixed background that may have differed from that in the present point-mutated mice. In addition, the present mice did not show any signs of inflammation in any organ, consistent with observations in human non-neuronopathic Gaucher disease. The

origin of the inflammatory areas and molecules in the *gba*$^{L444P/L444P}$Ugcg$^{+/KO}$ mice is uncertain.

Differential residual GCase activities were observed in the CNS and visceral tissues of the Gaucher disease mice. Neuronopathic disease is the life-threatening complication in the human types 2 and 3 variants.[1] Few studies of residual GCase activity are available on fresh brains of such affected patients.[42,43] Mouse models could be helpful in understanding the basis of the neuronopathic disease. An unexpected finding was the >2-fold greater residual activities in brain (21 to 28%) compared to those in visceral organs (~2.5 to 11%) from the respective point-mutant mice. These activities were obtained in the presence of CBE to minimize potential contributions from non-GCase β -glucosidase activities in the assessments. Glucosylceramide accumulation was not evident in the CNS of *gba* mutant mice. Furthermore, none of these mice up to >1 yr showed observable neuronopathic involvement phenotypically or histologically. The basis for the differential, and potentially protective, residual GCase activity is not evident, particularly since tissue mRNA GCase levels of these point-mutant GCase were similar to those in WT mice. This suggests a differential in post-translational processing or lower turnover of mutant GCase protein in brain than in other tissue types.

In visceral tissues the appearance of storage cells was not directly correlated with the *in vitro* level of residual GCase activity. In all three homozygous mutant mice and their respective compound heterozygotes, the livers had lower residual activities and fewer storage cells or stored lipid than the spleen or lung. In the D409V/null mice, the residual GCase activity in lung (4.0%) was similar to that in liver (3.9%), but larger numbers of storage cells were found in lung. These observations indicate a different threshold level for residual activity in different tissue type and/or different levels of glucosylceramide presentation to the liver and lung.

An important issue in studies of *gba* point-mutated mouse models is the correspondence with human diseases and hGCases. In particular, the lethality of the N370S/N370S mice was unexpected since humans with this genotype characteristically have less severe disease.[7] The mouse N370S and V394L enzymes expressed in the baculovirus systems had inhibition analyses with CBE that were similar to the human N370S and V394L (ie, a 3- to 5-fold increased IC_{50}). Also, hGCase and mGCase have similar thermostabilities (data not shown).

The skin of N370S/N370S or N370S/null pups appeared similar to that in the GCase-null or L444P-like homozygote pups. This suggests a skin permeability barrier defect in these mice as the cause of demise. This phenotype did not correlate with the level of *in vitro* residual activity in cultured skin fibroblasts (~13% of WT). This implies that mouse N370S GCase may not efficiently degrade the skin glucosylceramides with very long chain fatty acid acyl chains as well as the hGCase N370S. Further study of lipid metabolism in these point-mutated mice *in vivo* or *ex vivo* will be necessary to understand this pathophysiology.

In humans D409H homozygosity is associated with a characteristic phenotype of aortic root and valve calcification as well as progressive CNS abnormalities.[44] However, these pathological changes were not found grossly in the few D409H/D409H mice or more severe D409H/null mice examined to date. D409V has been found only as a heteroallelic mutation in humans with type 1 and 3 diseases.[10,45] In mice D409V/D409V leads to a more severe phenotype than the D409H/D409H. GCase activity in D409V/null mice was insufficient to clear glucosylceramide from the lungs leading to a significant number of storage cells in that organ early in life.

Overall, mGCases (ie, WT and N370S) have similar biochemical properties as their human counterpart. However, the tissue involvement in GCase point-mutated mice showed phenotypic and histological differences from the human counterparts. This may suggest the different physiology of mGCase *in vivo* and different balance of between GSL synthetic and degradation pathways in mouse compared with in human. Although there are some differences in phenotypes in Gaucher patients and in point-mutated mice, these viable mice should provide for pathophysiologic and therapeutic studies *in vivo*.

Acknowledgments

We thank Maryann Koenig for her clerical expertise and to Michael Craig, Dr. Huiquan Zhao, Andrej Kazimierczuk, Chris Woods, and Lisa McMillin for their excellent technical assistance.

References

1. Beutler E, Grabowski GA: Gaucher disease. The Metabolic and Molecular Bases of Inherited Diseases. Edited by Scriver CR, Beaudet AL, Sly WS, Valle D. New York, McGraw-Hill, 2001, pp 3635–3668
2. Blom S, Erikson A: Gaucher disease–Norrbottnian type: neurodevelopmental, neurological, and neurophysiological aspects. Eur J Pediatr 1983, 140:316–322
3. Kolodny EH, Ullman MD, Mankin HJ, Raghavan SS, Topol J, Sullivan JL: Phenotypic manifestations of Gaucher disease: clinical features in 48 biochemically verified type 1 patients and comment on type 2 patients. Prog Clin Biol Res 1982, 95:33–65
4. Volk BW, Wallace BJ, Adachi M: Infantile Gaucher's disease: electron microscopic and histochemical studies of a cerebral biopsy. J Neuropathol Exp Neurol 1967, 26:176–177
5. Adachi M, Wallace BJ, Schneck L, Volk BW: Fine structure of central nervous system in early infantile Gaucher's disease. Arch Pathol (Chicago) 1967, 83:513–526
6. Charrow J, Andersson HC, Kaplan P, Kolodny E, Mistry PK, Pastores G, Rosenbloom B, Scott CR, Wappner RS, Weinreb N, Zimran A: The Gaucher registry: demographics and disease characteristics of 1698 patients with Gaucher disease. Arch Intern Med 2000, 160:2835–2843
7. Sibille A, Eng CM, Kim SJ, Pastores G, Grabowski GA: Phenotype/genotype correlations in Gaucher disease type I: clinical and therapeutic implications. Am J Hum Genet 1993, 52:1094–1101
8. Abrahamov A, Elstein D, Gross-Tsur V, Farber B, Glaser Y, Hadas-Halpern I, Ronen S, Tafakjdi M, Horowitz M, Zimran A: Gaucher's disease variant characterised by progressive calcification of heart valves and unique genotype. Lancet 1995, 346:1000–1003
9. Theophilus B, Latham T, Grabowski GA, Smith FI: Gaucher disease: molecular heterogeneity and phenotype-genotype correlations. Am J Hum Genet 1989, 45:212–225
10. Theophilus BD, Latham T, Grabowski GA, Smith FI: Comparison of

RNase A, a chemical cleavage and GC-clamped denaturing gradient gel electrophoresis for the detection of mutations in exon 9 of the human acid β-glucosidase gene. Nucleic Acids Res 1989, 17:7707–7722
11. Grace ME, Newman KM, Scheinker V, Berg-Fussman A, Grabowski GA: Analysis of human acid β-glucosidase by site-directed mutagenesis and heterologous expression. J Biol Chem 1994, 269:2283–2291
12. Sidransky E, Tayebi N, Stubblefield BK, Eliason W, Klineburgess A, Pizzolato GP, Cox JN, Porta J, Bottani A, DeLozier-Blanchet CD: The clinical, molecular, and pathological characterisation of a family with two cases of lethal perinatal type 2 Gaucher disease. J Med Genet 1996, 33:132–136
13. Finn LS, Zhang M, Chen SH, Scott CR: Severe type II Gaucher disease with ichthyosis, arthrogryposis, and neuronal apoptosis: molecular and pathological analyses. Am J Med Genet 2000, 91:222–226
14. Tayebi N, Cushner SR, Kleijer W, Lau EK, Damschroder-Williams PJ, Stubblefield BK, Den Hollander J, Sidransky E: Prenatal lethality of a homozygous null mutation in the human glucocerebrosidase gene. Am J Med Genet 1997, 73:41–47
15. Tybulewicz VLJ, Tremblay ML, LaMarca ME, Willemsen R, Stubblefield BK, Winfield S, Zablocka B, Sidransky E, Martin BM, Huang SP, Mintzer KA, Westphal H, Mulligan RC, Ginns EI: Animal model of Gaucher's disease from targeted disruption of the mouse glucocerebrosidase gene. Nature 1992, 357:407–410
16. Liu Y, Suzuki K, Reed JD, Grinberg A, Westphal H, Hoffmann A, Doring T, Sandhoff K, Proia RL: Mice with type 2 and 3 Gaucher disease point mutations generated by a single insertion mutagenesis procedure. Proc Natl Acad Sci USA 1998, 95:2503–2508
17. Kyle JW, Birkenmeier EH, Gwynn B, Vogler C, Hoppe PC, Hoffmann JW, Sly WS: Correction of murine mucopolysaccharidosis VII by a human β-glucuronidase transgene. Proc Natl Acad Sci USA 1990, 87:3914–3918
18. Vogler C, Birkenmeier EH, Sly WS, Levy B, Pegors C, Kyle JW, Beamer WG: A murine model of mucopolysaccharidosis VII: gross and microscopic findings in β-glucuronidase-deficient mice. Am J Pathol 1990, 136:207–217
19. Sands MS, Barker JE, Vogler C, Levy B, Gwynn B, Galvin N, Sly WS, Birkenmeier E: Treatment of murine mucopolysaccharidosis type VII by syngeneic bone marrow transplantation in neonates. Lab Invest 1993, 68:676–686
20. Clarke LA, Russell CS, Pownall S, Warrington CL, Borowski A, Dimmick JE, Toone J, Jirik FR: Murine mucopolysaccharidosis type I: targeted disruption of the murine α-L-iduronidase gene. Hum Mol Genet 1997, 6:503–511
21. de Geest N, Bonten E, Mann L, de Sousa-Hitzler J, Hahn C, d'Azzo A: Systemic and neurologic abnormalities distinguish the lysosomal disorders sialidosis and galactosialidosis in mice. Hum Mol Genet 2002, 11:1455–1464
22. Marathe S, Miranda SR, Devlin C, Johns A, Kuriakose G, Williams KJ, Schuchman EH, Tabas I: Creation of a mouse model for non-neurological (type B) Niemann-Pick disease by stable, low level expression of lysosomal sphingomyelinase in the absence of secretory sphingomyelinase: relationship between brain intra-lysosomal enzyme activity and central nervous system function. Hum Mol Genet 2000, 9:1967–1976
23. Li CM, Park JH, Simonaro CM, He X, Gordon RE, Friedman AH, Ehleiter D, Paris F, Manova K, Hepbildikler S, Fuks Z, Sandhoff K, Kolesnick R, Schuchman EH, Hepbiloikler S: Insertional mutagenesis of the mouse acid ceramidase gene leads to early embryonic lethality in homozygotes and progressive lipid storage disease in heterozygotes. Genomics 2002, 79:218–224
24. Sandhoff K, Kolter T, Harzer K: Sphingolipid activator proteins. The Metabolic and Molecular Bases of Inherited Disease. Edited by Scriver CR, Beaudet A, Sly W, Valle D. New York, McGraw-Hill, 2001, pp 3371–3388
25. Dahl N, Lagerström M, Erikson A, Pettersson U: Gaucher disease type III (Norrbottnian type) is caused by a single mutation in exon 10 of the glucocerebrosidase gene. Am J Hum Genet 1990, 47:275–278
26. Lewis BD, Nelson PV, Robertson EF, Morris CP: Mutation analysis of 28 Gaucher disease patients: the australasian experience. Am J Med Genet 1994, 49:218–223
27. O'Neill RR, Tokoro T, Kozak CA, Brady RO: Comparison of the chromosomal localization of murine and human glucocerebrosidase genes and of the deduced amino acid sequences. Proc Natl Acad Sci USA 1989, 86:5049–5053
28. Sambrook J, Fritsch EF, Maniatis T: Molecular Cloning, A Laboratory Manual. New York, Cold Spring Harbor Laboratory, 1989
29. Sabath DE, Broome HE, Prystowsky MB: Glyceraldehyde-3-phosphate dehydrogenase mRNA is a major interleukin 2-induced transcript in a cloned T-helper lymphocyte. Gene 1990, 91:185–191
30. Ausubel FM, Brent R, Kingston RE, Moore DD, Seidman JG, Smith JA, Struhl K: Current Protocols in Molecular Biology. New York, Greene Publishing Associates and Wiley-Interscience, 1992, pp 10.5.1–10.5.5
31. Fabbro D, Desnick RJ, Grabowski GA: Gaucher disease: genetic heterogeneity within and among the subtypes detected by immunoblotting. Am J Hum Genet 1987, 40:15–31
32. O'Reilly DR, Miller LK, Luckow VA: Baculovirus Expression Vectors: A Laboratory Manual. New York, W. H. Freeman and Company, 1992
33. Grabowski GA, Osiecki-Newman K, Dinur T, Fabbro D, Legler G, Gatt S, Desnick RJ: Human acid β-glucosidase: use of conduritol B epoxide derivatives to investigate the catalytically active normal and Gaucher disease enzymes. J Biol Chem 1986, 261:8263–8269
34. Fujita N, Suzuki K, Vanier MT, Popko B, Maeda N, Klein A, Henseler M, Sandhoff K, Nakayasu H: Targeted disruption of the mouse sphingolipid activator protein gene: a complex phenotype, including severe leukodystrophy and wide-spread storage of multiple sphingolipids. Hum Mol Genet 1996, 5:711–725
35. Wells MA, Dittmer JC: The use of Sephadex for the removal of non-lipid contaminants from lipid extracts. Biochemistry 1963, 2:1259–1263
36. Dreyfus H, Guerold B, Freysz L, Hicks D: Successive isolation and separation of the major lipid fractions including gangliosides from single biological samples. Anal Biochem 1997, 249:67–78
37. Igisu H, Takahashi H, Suzuki K, Suzuki K: Abnormal accumulation of galactosylceramide in the kidney of twitcher mouse. Biochem Biophys Res Commun 1983, 110:940–944
38. Daniels LB, Coyle PJ, Glew RH, Radin NS, Labow RS: Brain glucocerebrosidase in Gaucher's disease. Arch Neurol 1982, 39:550–556
39. Mizukami H, Mi Y, Wada R, Kono M, Yamashita T, Liu Y, Werth N, Sandhoff R, Sandhoff K, Proia RL: Systemic inflammation in glucocerebrosidase-deficient mice with minimal glucosylceramide storage. J Clin Invest 2002, 109:1215–1221
40. Sauer B: Inducible gene targeting in mice using the Cre/lox system. Methods 1998, 14:381–392
41. Conzelmann E, Sandhoff K: Partial enzyme deficiencies: residual activities and the development of neurological disorders. Dev Neurosci 1983, 6:58–71
42. Svennerholm L, Hakansson G, Mansson JE, Nilsson O: Chemical differentiation of the Gaucher subtypes. Prog Clin Biol Res 1982, 95:231–252
43. Conradi NG, Sourander P, Nilsson O, Svennerholm L, Erikson A: Neuropathology of the Norrbottnian type of Gaucher disease: morphological and biochemical studies. Acta Neuropathol (Berl) 1984, 65:99–109
44. Pasmanik-Chor M, Laadan S, Elroy-Stein O, Zimran A, Abrahamov A, Gatt S, Horowitz M: The glucocerebrosidase D409H mutation in Gaucher disease. Biochem Mol Med 1996, 59:125–133
45. Latham TE, Theophilus BD, Grabowski GA, Smith FI: Heterogeneity of mutations in the acid β-glucosidase gene of Gaucher disease patients. DNA Cell Biol 1991, 10:15–21